Journal of Biomedical Optics

SPIEDigitalLibrary.org/jbo

Hyperspectral imaging for early detection of oxygenation and perfusion changes in irradiated skin

Michael S. Chin
Brian B. Freniere
Yuan-Chyuan Lo
Jonathan H. Saleeby
Stephen P. Baker
Heather M. Strom
Ronald A. Ignotz
Janice F. Lalikos
Thomas J. Fitzgerald

SPIE

Hyperspectral imaging for early detection of oxygenation and perfusion changes in irradiated skin

Michael S. Chin, Brian B. Freniere, Yuan-Chyuan Lo, Jonathan H. Saleeby, Stephen P. Baker, Heather M. Strom, Ronald A. Ignotz, Janice F. Lalikos, and Thomas J. Fitzgerald
University of Massachusetts Medical School, 55 Lake Avenue North, Worcester, Massachusetts 01655

Abstract. Studies examining acute oxygenation and perfusion changes in irradiated skin are limited. Hyperspectral imaging (HSI), a method of wide-field, diffuse reflectance spectroscopy, provides noninvasive, quantified measurements of cutaneous oxygenation and perfusion. This study examines whether HSI can assess acute changes in oxygenation and perfusion following irradiation. Skin on both flanks of nude mice ($n = 20$) was exposed to 50 Gy of beta radiation from a strontium-90 source. Hyperspectral images were obtained before irradiation and on selected days for three weeks. Skin reaction assessment was performed concurrently with HSI. Desquamative injury formed in all irradiated areas. Skin reactions were first seen on day 7, with peak formation on day 14, and resolution beginning by day 21. HSI demonstrated increased tissue oxygenation on day 1 before cutaneous changes were observed ($p < 0.001$). Further increases over baseline were seen on day 14, but returned to baseline levels by day 21. For perfusion, similar increases were seen on days 1 and 14. Unlike tissue oxygenation, perfusion was decreased below baseline on day 21 ($p < 0.002$). HSI allows for complete visualization and quantification of tissue oxygenation and perfusion changes in irradiated skin, and may also allow prediction of acute skin reactions based on early changes seen after irradiation. [DOI: 10.1117/1.JBO.17.2.026010]

Keywords: hyperspectral imaging; spectroscopy; radiation; radiodermatitis; perfusion; skin.

Paper 11476L received Sep. 1, 2011; revised manuscript received Dec. 16, 2011; accepted for publication Dec. 20, 2011; published online Mar. 5, 2012.

1 Introduction

Ionizing radiation exposure can have profound biological consequences to skin and underlying subcutaneous tissue. Historically, concerns have focused on cutaneous injury secondary to radiotherapy, which can lead to skin damage, fibrosis, and wound healing complications. Other potential exposures include "dirty bomb" detonations and nuclear accidents, such as Chernobyl.[1,2] The recent events in the Fukushima Prefecture of Japan[3] have highlighted the need for the development of noninvasive and rapid techniques to evaluate patients for potential ionizing radiation exposure. Radiological attacks or accidents often do not allow for appropriate implementation of dosimetry strategies, and current tests for determining total dose exposure in a post-hoc fashion require technical expertise and do not generate real-time results.[4]

Ionizing radiation is known to induce a dose-dependent cascade of acute effects on the skin, collectively known as radiation dermatitis, that includes a progression of skin injury from erythema to more serious moist desquamation and ulceration. Long-term radiation-induced cutaneous complications include fibrosis, atrophy, induration, and secondary malignancy.[5]

Studies examining acute oxygenation and perfusion changes (<1 month) in irradiated fields are limited. Two current modalities used to evaluate these parameters are laser Doppler flowmetry (LDF) and transcutaneous oxygen-tension probes. Hyperspectral imaging (HSI) is a technology that has recently found various applications in the biomedical field, including assessments of diabetic foot ulcers and peripheral vascular disease.[6,7] Additionally, HSI has been used in murine and porcine models to study cutaneous perfusion during mechanical stress and hemorrhagic shock, respectively.[8,9] HSI is a method of wide-field diffuse reflectance spectroscopy that utilizes a spectral separator to vary the wavelength of light entering a digital camera and provides a diffuse reflectance spectrum for every pixel. These spectra are then compared to standard transmission solutions to calculate the concentration of oxyhemoglobin (Hb-oxy) and deoxyhemoglobin (Hb-deoxy) in each pixel, from which spatial maps of tissue oxygenation are constructed as previously described by Yudovsky *et al.*[10] OxyVu™-2 (HyperMed™, Inc. Greenwich, Connecticut) is a commercially available device that generates tissue oxygenation maps of the subpapillary plexus. This modality provides simultaneous measurements of cutaneous tissue oxygenation and perfusion that is both noninvasive and reproducible.

HSI may allow for rapid and effective evaluation of acute cutaneous injury following irradiation. The aim of the current study is to examine the ability of HSI to assess cutaneous changes in oxygenation and perfusion during the acute period following irradiation.

2 Methods

2.1 *Animals*

All experiments were performed in accordance with our Institutional Animal Care and Use Committee guidelines. Ten 8-week-old male SKH1-E hairless mice (Charles River Laboratories, Wilmington, Massachusetts)[11] were used. This mouse strain

Address all correspondence to: Michael S. Chin, Division of Plastic Surgery, University of Massachusetts Medical School, 55 Lake Avenue North, Worcester, Massachusetts 01655. Tel: 5088563723; Fax: 5088565250; E-mail: mchin.md@gmail.com.

0091-3286/2012/$25.00 © 2012 SPIE

is immunocompetent and amelanotic. For procedures, mice were anesthetized using a mixture of ketamine and xylazine. Eight tattoo marks were placed with a 29-gauge needle circumferentially around the area of the flank to be irradiated to allow for precise sequential scanning of the same area.

2.2 *Irradiation*

Irradiation protocol and dosimetry was based on a previously published model.[12] Mice were placed longitudinally in the lateral decubitus position on the base of a standard burette stand. The bottom end of an acrylic tube was positioned flush against the skin of the flank and secured to the stand with a standard burette clamp. A guide was placed at the top of the acrylic tube to ensure exact positioning of the source on the flank within the tube. Mice were exposed to a beta-radiation dose using a 13-mm-diameter strontium-90 source (GE Healthcare, Little Chalfont, United Kingdom). The active diameter of the source was 9 mm, with areas beyond this receiving no ionizing radiation. The target dose was 50 Gy at a depth of 95 μm in the skin with less than 10% of the total dose penetrating beyond 3.6 mm. This procedure was repeated to create bilateral flank wounds for a total of 20 wounds in 10 mice.

2.3 *Hyperspectral Imaging*

Spatial maps of tissue oxygenation were generated using a commercially available HSI system (OxyVu^{TM}-2, HyperMed^{TM}, Inc.). The general optical properties of this device have been previously described.[13] A narrowband-pass, liquid-crystal tunable filter (LCTF-10-20, CRI, Inc. Hopkinton, Massachusetts) was used to vary the wavelength of light passed on to a digital imaging detector (Guppy F-146B, Allied Vision Technologies, Stadtroda, Germany) to provide many images at 15 select wavelengths between 500 and 660 nm. Broadband light-emitting diodes were used to illuminate the sample (LUXEON, Philips Lumiled, Inc. San Jose, California). Twenty-second scans of tissue samples were obtained at a 17-inch focal distance. Data were analyzed online using a fiducial target to achieve spectral decomposition and two-dimensional image registration techniques.[10] Diffuse reflectance tissue spectra were determined for each pixel within this collection of images using proprietary algorithms. Using standard spectra for Hb-oxy and Hb-deoxy to decompose a 79-pixel-diameter region, mean Hb-oxy and Hb-deoxy values of the irradiated area were obtained. False color images were created to demonstrate tissue oxygenation spatially. The spatial resolution of the Hb-oxy and Hb-deoxy images was 60 μm. Perfusion was measured as total hemoglobin (tHb), which was calculated as the sum of Hb-oxy and Hb-deoxy. Tissue oxygenation (StO_2) was calculated as Hb-oxy divided by tHb. Hb-oxy, Hb-deoxy, and tHb are reported as arbitrary values that have previously been shown to correlate well with respective *in vivo* molar concentrations.[10]

Prior to imaging, the system was calibrated to a reference card (CheckPad^{TM}, HyperMed^{TM}, Inc.) for all acquisitions, and pixel reflectance was determined relative to this standard reflectance. A fiducial target was used to correct for motion artifact from respiratory effort. The mice were then placed in the lateral decubitus position on black background that was positioned over a heated 38 °C blanket (T/Pump®, Gaymar Industries, Inc. Orchard Park, New York). Mice were anesthetized for image acquisition. Wounds were left untreated for image acquisition.

Imaging was obtained immediately before irradiation on day 0, within 2 hours following irradiation, and then on days 1, 2, 3, 4, 7, 9, 11, 14, 16, 18, and 21. Image processing was conducted following image acquisition. Tattoo marks placed prior to irradiation were visible in the generated tissue oxygenation maps and allowed for serial tissue oxygenation measurements of the irradiated area to be made using the OxyVu^{TM}-2 user interface. Similar serial measurements were also performed on flank skin outside the irradiated field to serve as an internal control.

2.4 *Skin Assessment*

Skin reaction assessment was performed by two independent, blinded observers using visible images captured by the OxyVu^{TM}-2 system at the same time that HSI images were obtained. The method used to score the skin's acute reaction to ionizing radiation is based on a scale used by Randall and Coggle,[14] with a score of 0 representing normal skin, 1 representing erythema, 2 representing dry desquamation and/or pigmentation changes, 3 representing incomplete moist desquamation, and 4 representing complete moist desquamation.

3 Statistical Methods

Plots of oxygenation and perfusion data are expressed as the mean ± standard deviation. Differences in outcomes between time points were evaluated using general mixed linear models given repeated measures.[15] In the presence of significant time effects, pairwise comparisons were made using Fisher's least significant difference (LSD) multiple-comparisons procedure without multiplicity adjustments.[16] Compliance with the distributional assumption of normality was evaluated using the Kolmogorov-Smirnov one-sample, goodness of fit test for normality applied to model residuals. Calculations were performed using the Proc Mixed procedure of the SAS® Statistical Software package (SAS Institute, Inc. Cary, North Carolina). Statistical significance was assumed when p was less than 0.05.

4 Results

There was 100% response in all irradiated areas ($n = 20$). Seventeen areas developed moist desquamation, and three resulted in dry desquamation. No systematic difference in HSI signal was observed between areas of dry and moist desquamation. Skin reactions were first visible on day 7, with peak formation on day 14, and resolution beginning by day 21. Mean skin reaction scores are displayed in Fig. 1.

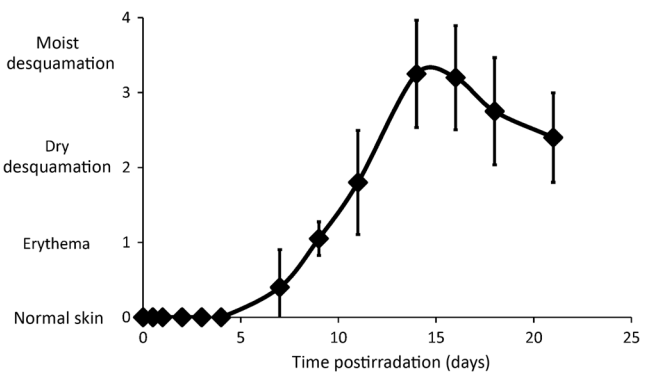

Fig. 1 Mean skin reaction scores (arbitrary units) as a function of time after a localized 50-Gy dose of beta-irradiation to the skin.

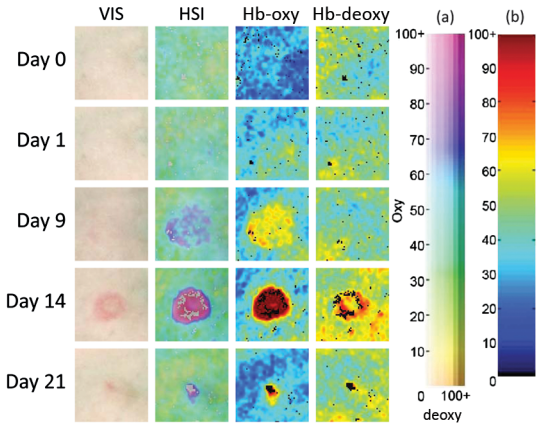

Fig. 2 Visible (VIS), hyperspectral selective (HSI), oxyhemoglobin selective (Hb-oxy), and deoxyhemoglobin selective (Hb-deoxy) windows on select days following irradiation for a representative subject. 1×1-cm^2 areas are reproduced 100% to scale. A dual-axis scale for interpretation of the HSI window is provided (a). For Hb-oxy and Hb-deoxy windows, a single axis scale is provided (b).

Spatial maps of tissue oxygenation demonstrated changes following irradiation (Fig. 2). These spatial maps were analyzed to yield mean Hb-oxy and Hb-deoxy levels over time [Figs. 3(a) and 3(b)]. From these values, mean tissue oxygen saturation and total hemoglobin levels were derived [Figs. 3(c) and 3(d)]. Compared to pre-irradiation day 0 values, tissue oxygen saturation was significantly increased over baseline by day 1 ($p < 0.001$). Tissue oxygen saturation remained elevated above baseline through day 21 ($p < 0.05$ for all times except 2 hours post-irradiation). Post-irradiation changes demonstrated two relative peaks of tissue oxygen saturation over surrounding days. Tissue oxygen saturation on day 1 was increased by 30% over baseline, after which there was a plateau with oxygen saturation values consistently 20% above baseline until day 7. A second and more prominent peak in oxygen saturation occurred at day 9 where oxygenation levels increased 42% relative to baseline. Following this second peak, there was a gradual return to near baseline by day 21.

When compared to the pre-irradiation day 0 values, mean total hemoglobin was significantly increased over baseline by day 1 ($p < 0.02$). Post-irradiation trends were similar to those for tissue oxygen saturation beginning with a peak at 10% above baseline by day 1. Total hemoglobin levels also increased a second time starting on day 9 and were 20% above baseline on day 14 ($p < 0.001$). Interestingly, not only did tHb levels begin to decrease back to baseline after the second peak in a pattern similar to tissue oxygen saturation, but also dropped below baseline levels by day 21 ($p < 0.002$).

In areas of non-irradiated flank skin, no significant changes in mean Hb-oxy and Hb-deoxy levels, from which oxygen saturation and total hemoglobin values are derived, were detected over the 21 days of observation [Figs. 4(a) and 4(b)].

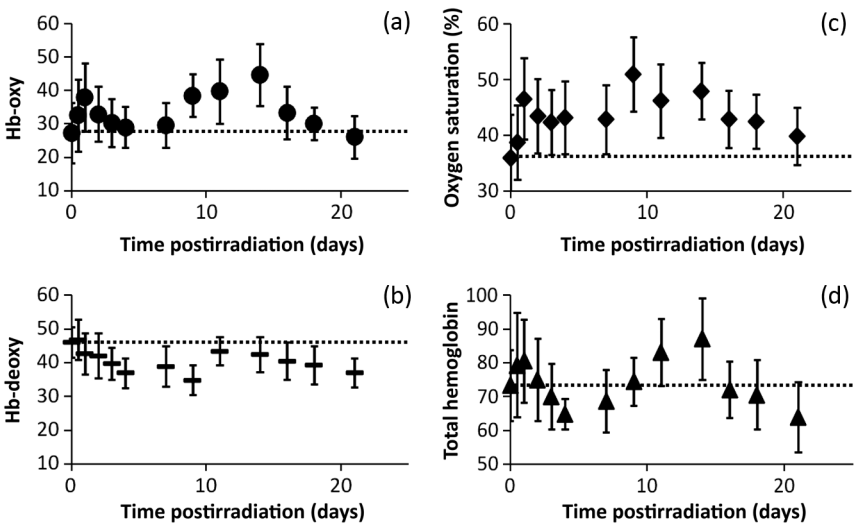

Fig. 3 Mean oxygen saturation (a), total hemoglobin (b), Hb-oxy (c), and Hb-deoxy (d) as a function of time after irradiation. Error bars are displayed representing ± standard deviation. Dashed lines represent baseline values in each plot, respectively.

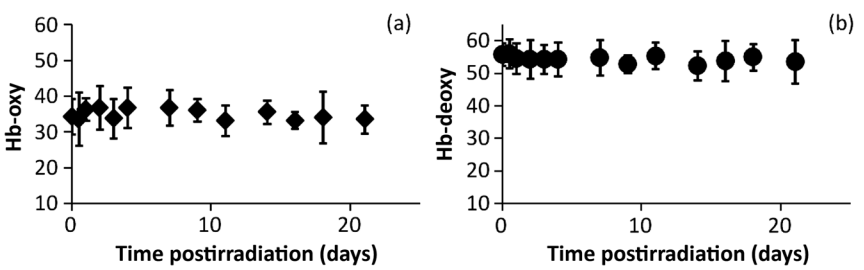

Fig. 4 Mean Hb-oxy (a) and Hb-deoxy (b) levels in non-irradiated skin as a function of time after flank skin irradiation. Error bars are displayed representing ± standard deviation.

5 Discussion

The pathophysiology of radiation-induced skin changes remains elusive. Prevailing theories suggest that the etiology may be the result of direct cellular injury,[17] cellular signaling pathway dysregulation,[18] or ischemia.[19] The literature examining whether radiation-induced skin damage is primarily mediated by vascular effects has generally focused on perfusion changes beyond 12 months. Studies examining acute perfusion changes (<1 month) are limited.

The most direct measurement of tissue oxygenation is by tonometry. Aitasalo and Aro describe early post-irradiation (days 1 and 35) hypoxia in the subcutaneous tissue of a rabbit hind limb utilizing surgically implanted tissue tonometers to directly measure tissue oxygen tension.[20] In the acute period, it was found that oxygen tension was decreased. Less invasive strategies have employed transcutaneous oxygen sensors for the same purpose and demonstrated that irradiated skin maintains normal tissue oxygenation in patients at least one year after irradiation.[17] However, this technique is limited by its measurement of a small area and requirement to heat the skin for accurate diffusion of oxygen across the skin.

LDF has been proposed as an alternative to noninvasive monitoring of perfusion, but has yielded inconsistent results. Utilizing LDF, there has been evidence of an acute rise in cutaneous blood flow after doses of at least 20 Gy.[21] Other findings have indicated that perfusion was not decreased one year after radiation treatment for breast cancer.[22] However, LDF has also demonstrated that within six months of irradiation, microvasculature has a reduced response to a heat stress.[23] Qualitative LDF imaging has also been used to show a decrease in cutaneous perfusion for six weeks following irradiation.[24] The main disadvantage of LDF is that flow velocity is being used as a surrogate marker for perfusion. While this hypothesis often holds true for normal physiology, pathologic processes that may distort tissue architecture can alter the implied relationship between flow velocity and perfusion.[25]

From the above studies, it is evident that there are inconsistencies among these findings. There are two common factors that confound these studies: sampling bias and time to measurement. Both transcutaneous and LDF rely primarily on point probes for measurement. Such a method is prone to sampling bias as perfusion can differ greatly from site to site even within the same irradiated field. Timing of measurement is also critical since it is evident from our observations that both increases and decreases in oxygenation and perfusion can be seen in the acute period depending on the stage of skin reaction. Furthermore, a clear distinction must be made between measurement of tissue oxygenation versus perfusion as the two physiologies are related, but not identical.

In our study, HSI has been used effectively to demonstrate changes in irradiated skin. Unlike previous methods, HSI is not prone to sampling error and is able to reliably generate a complete map of tissue oxygenation over a relatively large area. In addition, HSI measures the Hb-oxy and Hb-deoxy content of the subpapillary plexus itself and thus provides simultaneous measurement of total hemoglobin and tissue oxygen saturation. As a result, it is not reliant on a single surrogate marker to make conclusions regarding tissue oxygenation and perfusion.

Our results support previous studies demonstrating an early rise in perfusion within the first few weeks.[21,26] However, none of these studies examined the patterns of perfusion change within this acute period. The ability of the OxyVu™-2 system to quantify Hb-oxy and Hb-deoxy levels permits simultaneous analysis of changes in tissue oxygen saturation and total hemoglobin content over time in the acute post-irradiation phase. The increase in both of these parameters within the first day suggests that local metabolic processes may be increasing local tissue oxygen demand in this very early phase of ionizing radiation injury. Hb-oxy levels appear responsible for these observed increases. Near the end of week one post-irradiation, total hemoglobin declines to below baseline levels despite tissue oxygen saturation remaining above pre-irradiation levels. This appears driven by declining Hb-deoxy levels and suggests a distinct alteration in local oxygen demand.

At the second peak near two weeks post-irradiation, oxygen saturation and total hemoglobin levels similar to the first peak are observed and indicate a possible change in local metabolic conditions that may be distinct from the very early process. It is important to note that unlike the first peak, both Hb-oxy and Hb-deoxy increase proportionally indicating an overall increase in blood volume. Following this second peak, a gradual decline in oxygenation levels and a more pronounced decrease in perfusion are observed. These appear to be the result of decreasing Hb-oxy values since Hb-deoxy values only modestly decline, which could suggest decreased arterial inflow.

6 Conclusions

HSI allows for complete visualization and quantification of oxygenation and perfusion changes in irradiated skin. Further confirmatory studies are needed that will permit longer follow-up and correlation of observed oxygenation and perfusion changes with histological and molecular analysis. HSI may be a vehicle to rapidly identify individuals exposed to ionizing radiation after a radiological attack or accident. Further investigation will need to elucidate key differences in the hyperspectral appearance of radiation-induced versus other cutaneous forms of injury. HSI may offer quantitative metrics to identify people exposed to higher doses of ionizing radiation well before the appearance of any dermal injury and permit appropriate triage to healthcare facilities.

Acknowledgments

We would like to thank Laura Cardin for her logistical support and Travis Zhang for his engineering expertise. Without their assistance, this project would not have been possible.

References

1. F. K. Chin, "Scenario of a dirty bomb in an urban environment and acute management of radiation poisoning and injuries," *Singapore Med. J.* **48**(10), 950–957 (2007).
2. A. Barabanova and D. P. Osanov, "The dependence of skin lesions on the depth-dose distribution from beta-irradiation of people in the Chernobyl nuclear power plant accident," *Int. J. Radiat. Biol.* **57**(4), 775–782 (1990).
3. A. Leelossy, R. Meszaros, and I. Lagzi, "Short and long term dispersion patterns of radionuclides in the atmosphere around the Fukushima Nuclear Power Plant," *J. Environ. Radioact.* **102**(1), 1117–1121 (2011).
4. J. P. Christodouleas et al., "Short-term and long-term health risks of nuclear-power-plant accidents," *N. Engl. J. Med.* **364**(24), 2334–2341 (2011).
5. A. Olascoaga et al., "Wound healing in radiated skin: pathophysiology and treatment options," *Int. Wound J.* **5**(2), 246–257 (2008).
6. L. Khaodhiar et al., "The use of medical hyperspectral technology to evaluate microcirculatory changes in diabetic foot ulcers and to predict clinical outcomes," *Diabetes Care* **30**(4), 903–910 (2007).

7. J. A. Chin, E. C. Wang, and M. R. Kibbe, "Evaluation of hyperspectral technology for assessing the presence and severity of peripheral artery disease," *J. Vasc. Surg.* **54**(6), 1679–1688 (2011).
8. M. S. Chin et al., "In vivo acceleration of skin growth using a servo-controlled stretching device," *Tissue Eng. Part C Methods* **16**(3), 397–405 (2010).
9. L. C. Cancio et al., "Hyperspectral imaging: a new approach to the diagnosis of hemorrhagic shock," *J. Trauma* **60**(5), 1087–1095 (2006).
10. D. Yudovsky, A. Nouvong, and L. Pilon, "Hyperspectral imaging in diabetic foot wound care," *J. Diabetes Sci. Technol.* **4**(5), 1099–1113 (2010).
11. B. S. Schaffer et al., "Immune competency of a hairless mouse strain for improved preclinical studies in genetically engineered mice," *Mol. Cancer Ther.* **9**(8), 2354–2364 (2010).
12. J. E. Coggle et al., "Nonstochastic effects of different energy beta emitters on the mouse skin," *Radiat. Res.* **99**(2), 336–345 (1984).
13. D. Yudovsky et al., "Monitoring temporal development and healing of diabetic foot ulceration using hyperspectral imaging," *J. Biophotonics* **4** (7–8), 565–576 (2011).
14. K. Randall and J. E. Coggle, "Expression of transforming growth factor-beta 1 in mouse skin during the acute phase of radiation damage," *Int. J. Radiat. Biol.* **68**(3), 301–309 (1995).
15. R. A. McLean, W. L. Sanders, and W. W. Stroup, "A unified approach to mixed linear models," *Am. Statistician* **45**(1), 54–64 (1991).
16. B. J. Winer, *Statistical Principles in Experimental Design*, McGraw-Hill, New York (1971).
17. R. Rudolph et al., "Normal transcutaneous oxygen pressure in skin after radiation therapy for cancer," *Cancer* **74**(11), 3063–3070 (1994).
18. M. Martin, J. Lefaix, and S. Delanian, "TGF-beta1 and radiation fibrosis: a master switch and a specific therapeutic target?," *Int. J. Radiat. Oncol. Biol. Phys.* **47**(2), 277–290 (2000).
19. R. E. Marx et al., "Relationship of oxygen dose to angiogenesis induction in irradiated tissue," *Am. J. Surg.* **160**(5), 519–524 (1990).
20. K. Aitasalo and H. Aro, "Irradiation-induced hypoxia in bones and soft tissues: an experimental study," *Plast. Reconstr. Surg.* **77**(2), 256–267 (1986).
21. H. I. Amols et al., "Acute radiation effects on cutaneous microvasculature: evaluation with a laser Doppler perfusion monitor," *Radiology* **169**(2), 557–560 (1988).
22. K. Benediktsson and L. Perbeck, "The influence of radiotherapy on skin circulation of the breast after subcutaneous mastectomy and immediate reconstruction," *Br. J. Plast. Surg.* **52**(5), 360–364 (1999).
23. C. Doll et al., "Functional assessment of cutaneous microvasculature after radiation," *Radiother. Oncol.* **51**(1), 67–70 (1999).
24. V. D. Thanik et al., "A novel mouse model of cutaneous radiation injury," *Plast. Reconstr. Surg.* **127**(2), 560–568 (2011).
25. B. Azizi et al., "The impact of cataract on the quantitative, non-invasive assessment of retinal blood flow," *Acta Ophthalmol.* **90**(1), e9–e12 (2012).
26. J. Nystrom et al., "Objective measurements of radiotherapy-induced erythema," *Skin Res. Technol.* **10**(4), 242–250 (2004).